

# Retrieval of Soil Moisture Using Sliced Regression Inversion Technique

Siddhant Gautam<sup>1</sup>, Sakees V. Chidambaram<sup>2</sup>, Niharika Gunturu<sup>3</sup>, and Uday K. Khankhoje<sup>1</sup>

<sup>1</sup>Electrical Engineering, Indian Institute of Technology Madras, India

<sup>2</sup>SFO Technologies, Kochi, India

<sup>3</sup>Physics, Indian Institute of Technology Madras, India

**Abstract**— A soil moisture (SM) retrieval algorithm, rooted in electromagnetic theory, is proposed and validated against synthetic data with good retrieval accuracy. The proposed Sliced Regression (SR) algorithm generates piece-wise linear fits to a data set obtained from a forward model, and then retrieves the soil moisture by applying a linear least-squares approach. This algorithm is compared against a widely employed semi-empirical inversion algorithm (SMART), and it is observed that better results are returned from the former. Performance of the proposed retrieval algorithm on single band and dual band (L and S-bands) retrieval is studied; and it is found dual band retrieval returns better retrieval results for SM, along with other soil surface parameters.

The proposed algorithm is employed on synthetically generated data-sets (generated using the Integral Equation Method as the forward model for ground scattering) for SM retrieval scenario considering all the primary influencers on backscatter into the model. To measure SM for vegetated terrain, vegetation is modelled as a collection of randomly oriented dielectric cylinders with radii and length specific to the vegetation. The overall backscatter is calculated as the sum of individual contributions from the ground, vegetation and their interactions. Having parameterized the vegetation forward model as above, we extend the SR to retrieve SM in the presence of vegetation.

## 1. INTRODUCTION

Soil moisture (SM) is an important parameter in various environmental studies, such as in building climate models in meteorology, crop yield forecasting and irrigation scheduling in agriculture and to predict early warnings of drought/ flooding in disaster management to name a few [1, 2]. Therefore there is a need to measure SM on a large scale, cost-effective and routine basis through microwave remote sensing via synthetic aperture radar (SAR). SM, here, refers to water content in the surface soil corresponding to few centimeters [3].

Over the past few decades, several studies have proposed various algorithms for SM retrieval from SAR data. These can be broadly classified into three groups namely: *theoretical* models, *semi-empirical* models, and *empirical* models [3]. Empirical models are based on specific datasets and implementation conditions (such as the sensor parameters) and suffer from severe drawbacks such as site-specific applicability. Semi-empirical models are built on experimental or simulated datasets, but are guided by trends based on theoretical models. They serve to be simplistic in comparison with theoretical models and site independent as opposed to empirical models. Some such models include [4, 5, 8]. Theoretical models built on a strong physical basis generally result in the most accurate SM retrieval but suffer from being complex and computationally intensive models, particularly for inversion.

Another challenge for SM retrieval lies in the formulation of the forward model. For instance, soil naturally has a heterogeneous vertical profile. However the original IEM developed by Fung et al. [7, 10] assumes soil to be a homogeneous dielectric without any variation in permittivity with depth. In this paper, to retrieve depth dependent moisture, we use the extended IEM model to incorporate a vertical soil moisture profile [11].

It is often necessary to retrieve SM from surfaces covered by vegetation — not just bare soil. Thus, it is essential to formulate the forward model to take into account the scattering by vegetation. One of the two main approaches for modeling vegetation is the Canopy Cloud Model [14] which models vegetation as a water cloud with droplets held in place by vegetative matter. It then proceeds to model the ‘canopy’ as a homogeneous dielectric slab and considers volume scattering to be the predominant phenomenon. However, we pursue the second approach [12], in which vegetation is modelled as a collection of lossy dielectric scatterers, while considering the contribution of scattering from multiple paths through the vegetation to the final backscatter direction.

## 2. THEORY

This section illustrates the dependence of the radar backscatter on various physical factors related to the soil and vegetation.

### 2.1. Bare Soil with Homogeneous Soil Profile

Radar backscatter coefficient ( $\sigma$ ) from a random rough surface primarily depends on the surface geometrical properties, quantified by (i) RMS surface height ( $h$ ), (ii) correlation length ( $l$ ), and (iii) on the surface electrical properties as quantified by the complex dielectric constant ( $\epsilon$ ) of the soil substrate. Here, we use the improved integral equation model ( $I^2EM$ ) which is an algorithm that computes the backscattering coefficient of a rough surface for a given operating wavelength  $\lambda$  having any combination of receive and transmit wave polarizations [6]. We use the Hallikainen dielectric model [9] to calculate complex permittivity from soil moisture.

### 2.2. Effects of Depth Dependent Moisture

The Improved Integral Equation Model ( $I^2EM$ ) assumes the soil profile to be homogeneous, i.e., moisture is constant with respect to depth. Instead, we model the soil profile as a piece-wise constant, multilayer dielectric surface in which the field encounters multiple reflections as shown in Fig. 1 due to varying soil permittivity. For this purpose, we assume an exponentially varying dielectric profile [11] for the soil, whose expression is given by

$$\epsilon_r(z) = 1 + \frac{2(\epsilon_{r0} - 1)}{1 + e^{-mz}}, \quad z \geq 0 \quad (1)$$

where  $m$  is the transition rate factor and  $\epsilon_{r0}$  is the dielectric constant of the topmost layer. To account for the depth dependence, we update the reflectivities in the  $I^2EM$  with the effective Fresnel reflection coefficients of scattering from the heterogeneous soil profile.

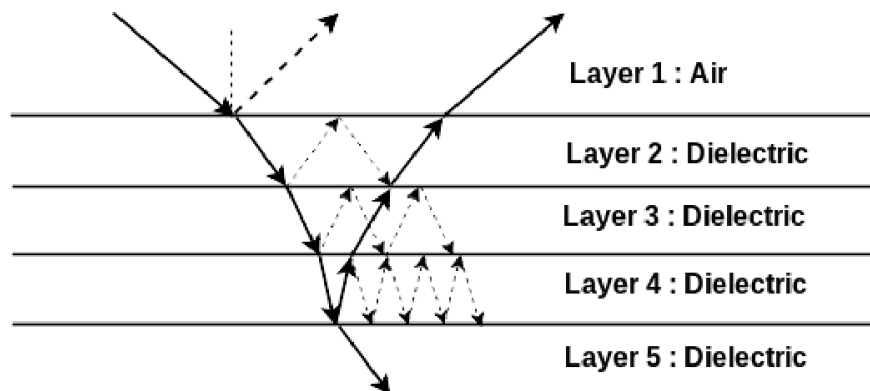


Figure 1. Multiple radar reflections from dielectric layers.

### 2.3. Effects of Vegetation Canopy

In most practical scenarios, there is a need to carry out soil moisture retrieval over vegetated terrain. In this paper, we model the vegetation as a layer consisting of a collection of randomly oriented dielectric cylinders. The spatial distribution of these cylinders are dictated by a suitable probability density function such that it mimics the true geometrical orientation of the vegetation [12, 13]. The dielectric constant of these cylinders accounts for contributions from free water, bound water and non-dispersive residues [15] :

$$\epsilon_v = \epsilon_r + v_{fw} \epsilon_f + v_b \epsilon_b \quad (2)$$

where  $\epsilon_v$  is the vegetation dielectric constant,  $\epsilon_r$  is the non-dispersive residual part of the dielectric constant,  $\epsilon_f$  and  $\epsilon_b$  are the dielectric constants of free water and bound water respectively while  $v_{fw}$  and  $v_b$  are the volume fraction of free water and vegetation bound water respectively.

Vegetation modelling varies greatly depending on the type of vegetation in question. Forests, for instance, are modelled as three or more layers of ‘primary’ and ‘secondary’ scatterers which include disks, needles and cylinders. Here, we are concerned with the modelling of agricultural crops and hence, as a reasonable first-order approximation, we model the vegetation as a single layer of

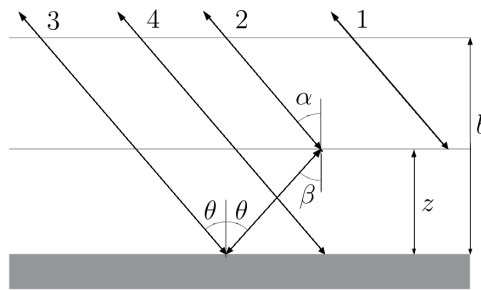


Figure 2. Scattering paths.

randomly oriented cylinders whose spatial distribution is cosine squared about the vertical [13]. In our approach, we ignore multiple scatterings apart from the case of double reflection. With this assumption, we can categorize any scattering into four different paths [16].

1. Scattering from the Vegetation Layer (Path 1)
2. Backscatter from the Ground Surface (Path 4)
3. Double Reflection Scattering (Paths 2 and 3)

For the case of Double Reflection Scattering, we model the scattering at the cylinder to be bistatic and the scattering at the ground to be specular. For backscatter from the ground surface — we incorporate the aforementioned  $I^2EM$  with depth dependence along with an attenuation term as specified in Eq. (3). Summing up the individual contributions from the four paths, the total backscatter coefficient is given by

$$\sigma_{total} = \sigma_{veg}(vwc, a, b, \rho_s) + \tau^2 \sigma_{IEM}(h, l, \epsilon) + \sigma_{db}(vwc, a, b, \rho_s, h, l, \epsilon) \quad (3)$$

where  $\tau^2$  is an attenuation coefficient which is a function of vegetation characteristics,  $vwc$  is the vegetation water content,  $b$  is the cylinder height,  $a$  is the cylinder radius and  $\rho_s$  is the density of scatterers.

### 3. METHODOLOGY

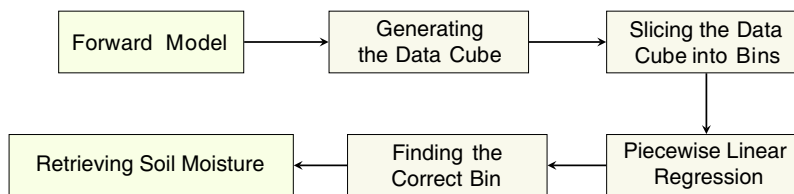


Figure 3. The flow of sub-tasks to retrieve SM through the sliced inversion regression algorithm.

The radar backscatter coefficient,  $\sigma$ , is a non-linear function of soil and vegetation parameters. This makes inversion for soil moisture (a function of  $\epsilon$ ) both a challenging and computationally intensive task. In this section, we describe our SM retrieval algorithm — the Sliced Regression Inversion technique. The proposed algorithm broadly consists of two parts — the forward and the inverse problem. The overall methodology of our algorithm is shown graphically in Fig. 3, and the individual steps of the algorithm are described below.

#### 3.1. Generating Data Cube

The forward model is employed to synthetically generate the radar backscatter ( $\sigma$ ) values for all combinations of physically plausible values of surface parameters ( $h, l, \epsilon$ ) and vegetation parameters ( $vwc, a, b, \rho_s$ ). Such a construct of a dataset is referred to as a ‘datacube’. For our algorithm, we generate six such datacubes corresponding to the three polarizations ( $\sigma^{hh}$ ,  $\sigma^{hv}$  and  $\sigma^{vv}$ ) for each of the two frequency bands (L & S-band). Notation-wise, in the case of  $\sigma^{pq.f}$ ,  $p, q$  refer to the transmitted and received signal polarization respectively (either  $H$  or  $V$  for horizontal and vertical polarization, respectively) at frequency band  $f$ .

### 3.2. Creating Bins

The next step is to partition the entire data cube into smaller bins. Due to the function nonlinearity, it was found that the model works best by partitioning the data cube into the smallest possible grids (or bins), though this has a higher computational price. Thus we partition the data cube by taking the adjacent data points as the end points of bin. Therefore, for an  $N$ -dimensional datacube, each bin will have  $2^N$  points. It is important to note that this is a one time effort and need not be repeated for multiple inversions.

### 3.3. Linear Regression

Once the datacube is partitioned into bins, we perform linear regression in each bin to obtain an  $N$  dimensional hyperplane between input and output parameters. Through this, we obtain, for each bin, the set of regression coefficients  $\beta_0, \beta_1, \dots, \beta_N$  from the radar backscatter values  $\sigma^{p,q,f}$  for *that* bin. We present the retrieval for a single crop type assuming the cylinder length, radius and density of scatterers to be constant. The linear relation between backscatter  $\sigma$  and input parameters can thus be given as:

$$\sigma = \beta_0 + \beta_1 h + \beta_2 l + \beta_3 m_v + \beta_4 m + \beta_5 vvc \quad (4)$$

The corresponding matrix equation is as follows:

$$\underbrace{\begin{bmatrix} \sigma_1^{hh,l} & \sigma_1^{vv,l} & \sigma_1^{hh,s} & \sigma_1^{vv,s} & \sigma_1^{hv,l} & \sigma_1^{hv,s} \\ \sigma_2^{hh,l} & \sigma_2^{vv,l} & \sigma_2^{hh,s} & \sigma_2^{vv,s} & \sigma_2^{hv,l} & \sigma_2^{hv,s} \\ \vdots & \vdots & \vdots & \vdots & \vdots & \vdots \\ \sigma_n^{hh,l} & \sigma_n^{vv,l} & \sigma_n^{hh,s} & \sigma_n^{vv,s} & \sigma_n^{hv,l} & \sigma_n^{hv,s} \end{bmatrix}}_{\mathbf{Y}} = \underbrace{\begin{bmatrix} 1 & h_1 & l_1 & mv_1 & m_1 & vvc_1 \\ 1 & h_2 & l_2 & mv_2 & m_2 & vvc_2 \\ \vdots & \vdots & \vdots & \vdots & \vdots & \vdots \\ 1 & h_n & l_n & mv_n & m_n & vvc_n \end{bmatrix}}_{\mathbf{X}} \underbrace{\begin{bmatrix} \beta_0^{hh,l} & \beta_0^{vv,l} & \dots & \beta_0^{hv,s} \\ \beta_1^{hh,l} & \beta_1^{vv,l} & \dots & \beta_1^{hv,s} \\ \vdots & \vdots & \ddots & \vdots \\ \beta_5^{hh,l} & \dots & \dots & \beta_5^{hv,s} \end{bmatrix}}_{\boldsymbol{\beta}} \quad (5)$$

The regression coefficients,  $\boldsymbol{\beta}$ , can be found by solving the equation  $\boldsymbol{\beta} = \mathbf{X}^+ \mathbf{Y}$  where  $\mathbf{X}^+$  is the pseudoinverse of  $\mathbf{X}$ . Fig. 4 shows a 2-dimensional datacube to illustrate the idea of hyperplanes.

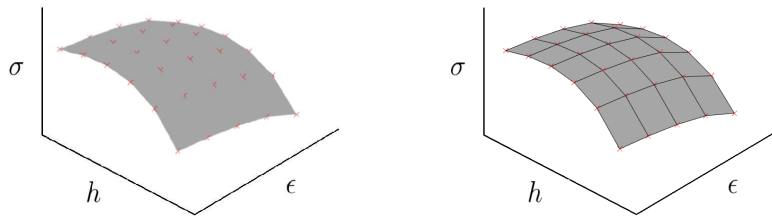


Figure 4. Partitioning the data cube into bins — the vertical axis represents the backscatter, while the horizontal axis represent the independent physical parameters. The left hand figure shows the actual backscatter function, with red dots indicating the discrete data points used to generate the data cube. The right figure shows the hyperplanes generated by performing linear regression on each sliced bin.

### 3.4. Inversion

After computing the regression coefficients,  $\boldsymbol{\beta}$ , we estimate the value of soil and vegetation parameters, i.e.,  $\boldsymbol{x}$ , using the radar backscatter ( $\sigma$ ) obtained from SAR data. The parameters ( $\boldsymbol{x}$ ) can be found by minimizing the cost function subject to the following constraints for *each* bin:

$$\begin{aligned} & \underset{\boldsymbol{x}}{\text{minimize}} && \|\boldsymbol{\beta}\boldsymbol{x} - \boldsymbol{y}\|_2^2 + \gamma \|\boldsymbol{x}_m\|_2^2 \\ & \text{subject to} && \mathbf{lb} \leq \boldsymbol{x} \leq \mathbf{ub} \quad \text{for each bin} \end{aligned} \quad (6)$$

where  $lb$ ,  $ub$  are the lower and upper bounds of each bin,  $\gamma$  is a regularization factor set empirically, and  $\mathbf{y}$  is defined as:

$$\underbrace{\begin{bmatrix} \sigma^{hh,l} - \beta_0^{hh,l} \\ \sigma^{vv,l} - \beta_0^{vv,l} \\ \sigma^{hh,s} - \beta_0^{hh,s} \\ \sigma^{vv,s} - \beta_0^{vv,l} \\ \sigma^{hv,l} - \beta_0^{hv,l} \\ \sigma^{hv,s} - \beta_0^{hv,s} \end{bmatrix}}_{\mathbf{y}} = \underbrace{\begin{bmatrix} \beta_1^{hh,l} & \beta_2^{hh,l} & \beta_3^{hh,l} & \beta_4^{hh,l} & \beta_5^{hh,l} \\ \beta_1^{vv,l} & \beta_2^{vv,l} & \beta_3^{vv,l} & \beta_4^{vv,l} & \beta_5^{vv,l} \\ \beta_1^{hh,s} & \beta_2^{hh,s} & \beta_3^{hh,s} & \beta_4^{hh,s} & \beta_5^{hh,s} \\ \beta_1^{vv,s} & \beta_2^{vv,s} & \beta_3^{vv,s} & \beta_4^{vv,s} & \beta_5^{vv,s} \\ \beta_1^{hv,l} & \beta_2^{hv,l} & \beta_3^{hv,l} & \beta_4^{hv,l} & \beta_5^{hv,l} \\ \beta_1^{hv,s} & \beta_2^{hv,s} & \beta_3^{hv,s} & \beta_4^{hv,s} & \beta_5^{hv,s} \end{bmatrix}}_{\boldsymbol{\beta}} \underbrace{\begin{bmatrix} h \\ l \\ mv \\ m \\ vvc \end{bmatrix}}_{\mathbf{x}} \quad (7)$$

and the regularization term  $\mathbf{x}_m = [0 \ 0 \ 0 \ m \ 0]^T$  forces the transition rate factor ( $m$ ) to have small value. For a given data point, we choose the bin which has the minimum error (as defined by Eq. (6)) and this bin is used for retrieval.

#### 4. RESULTS

In order to test the accuracy of the model, the root mean squared error (RMSE), relative percentage error, standard deviation (SD) and the correlation coefficient values ( $R$ ) are used. The correlation coefficient is a measure of the correlation relationship between the measurements and observations.

$$R = \frac{\text{Cov}(a, b)}{\sqrt{\text{Var}|a|\text{Var}|b|}} \quad (8)$$

$$\text{RMSE} = \sqrt{\frac{1}{N} \sum_{i=1}^N (a_i - b_i)^2} \quad (9)$$

$$\% \text{ error} = \sqrt{\frac{1}{N} \sum_{i=1}^N \left( \frac{a_i - b_i}{a_i} \right)^2} \times 100 \quad (10)$$

where  $a_i$  is the true value and  $b_i$  is the estimated value of the parameter and  $N$  is the number of data points. The standard deviation is calculated by taking the square root of variance, i.e.,  $\text{SD} = \sqrt{\text{Var}|a|}$ .

##### 4.1. Comparison with SMART Inversion Algorithm

We compare the retrieval results from SMART [8], a semi empirical soil inversion algorithm, with the proposed Sliced Regression Inversion algorithm. Both the inversion algorithms were run on the datacube obtained from the SMART Forward model. The comparison of retrieval results from both the methods (with an added noise of 0.6 dB) is tabulated below. From the results tabulated below, it is evident that the Sliced Regression Inversion algorithm gives more accurate results than the SMART algorithm for the retrieval of soil moisture ( $m_v$ ) as well as RMS height ( $h$ ).

Table 1. Comparison between SMART and proposed SR algorithm for SM retrieval.

Algorithm	h (cm)		$m_v$ ( $\text{cm}^3/\text{cm}^3$ )	
	RMSE	SD	RMSE	SD
<b>SR Inversion</b>	0.20	0.04	0.053	0.012
<b>SMART Inversion</b>	0.25	0.07	0.073	0.019

##### 4.2. Single-band vs Dual-band Retrieval Results

It is expected that operating SAR at two different frequencies will provide more information about the location being monitored as compared to a single frequency. To investigate the improvement in the retrieval accuracy for dual band operation, we conduct the following study. As in the previous section, the SMART Forward model is employed to populate the datacube in case of single-band (L) and dual-band (L & S). From the results, we infer that dual band retrieval is more accurate in case of all retrieval parameters.

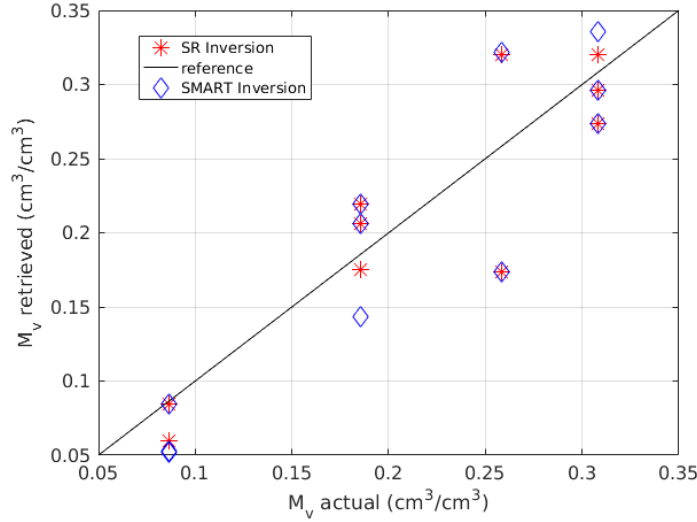


Figure 5. Comparison between SMART and proposed SR algorithm.

Table 2. Single and dual band comparison results for added noise of 0.6 dB.

Frequency	$h$ (cm)		$\epsilon$		$m_v$ ( $\text{cm}^3/\text{cm}^3$ )	
	RMSE	SD	RMSE	SD	RMSE	SD
Single band	0.19	0.05	3.28	0.88	0.053	0.015
Dual band	0.14	0.03	2.21	0.49	0.037	0.010

### 4.3. Bare Soil with Depth Dependent Moisture

For the case in which soil is assumed to have heterogeneous profile, i.e., depth dependent moisture, the retrieval is done using synthetically generated test data from the forward model. In case of bare soil, the cross polarization component of backscatter is not significant, thus we only use the co-polarization components of L and S band (i.e.,  $\sigma_{hh}$  and  $\sigma_{vv}$ ) for retrieval. The following ranges were selected for each of the parameters for generating the datacube:  $h = [0.3, 0.7, 1.5]$ ,  $l = [4, 18, 34]$ ,  $\epsilon_r = [3, 7, 12, 19]$ ,  $\epsilon_i = [0, 0.5, 1, 1.5]$ ,  $m = [0, 4, 8, 12]$ . We present the retrieval results for this case in the table below using the relative percentage error as the error metric. We also provide the results with retrieval done on a validation set with the errors summarized as below. For a general case of random test data with 0.5 dB added noise, we get a relative percentage error of 11.57 % in the soil dielectric constant  $\epsilon$ .

Table 3. Retrieval results (% error) for depth dependent moisture with (a) Validation &amp; (b) Random test data.

Noise level	$\epsilon$	$h$	$l$
0 dB	5.39	3.79	6.21
0.5 dB	6.76	9.43	22.88

Noise level	$\epsilon$	$h$	$l$
0 dB	11.43	4.7	11.53
0.5 dB	11.57	9.6	23.7

### 4.4. Vegetation Inversion Results

After including the effects of vegetation into our model, we apply our algorithm to retrieve soil moisture from vegetated terrain. We solve the optimization problem specified by Eq. (7) for the parameters as specified below.

It is generally observed that the correlation length is hard to determine experimentally and its measurement is highly susceptible to errors. Hence we present the results for both fixed and variable correlation length. The algorithm is tested on a synthetically generated test data with added Gaussian noise of zero mean and 0.5 dB variance. The retrieval results are presented in the Table 5. From the table it is clear that both the soil and vegetation moisture is retrieved with

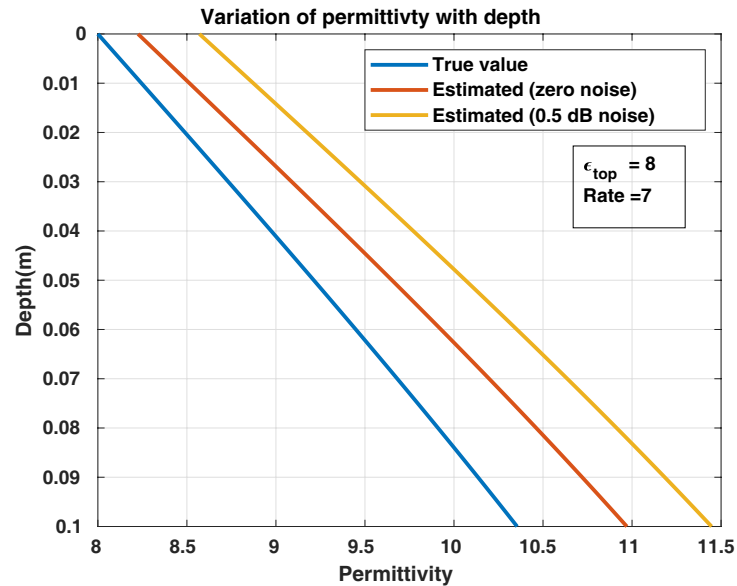


Figure 6. Soil profile with retrieved permittivity ( $\epsilon_{top} = 8$ ) and transition rate factor ( $m = 7$ ).

Table 4. (a) Fixed parameter values & (b) Parameter ranges for data cube generation.

Parameter	Value	Parameter	Range
Cylinder radius ( $a$ )	2 mm	RMS surface height ( $h$ )	0.3–1.7
Cylinder length ( $lc$ )	50 cm	Correlation length ( $l$ )	5–27
Cylinder density ( $\rho$ )	900 cylinders/m <sup>3</sup>	Soil moisture ( $m_v$ )	0.05–0.4
Vegetation layer height ( $b$ )	50 cm	Transition rate ( $m$ )	–6–6
Orientation PDF $p(\theta_c, \phi_c)$	$\cos^2 \theta_c \cos^2 \phi_c$	Vegetation Water Content ( $vwc$ )	0.15–0.4

good accuracy ( $< 10\%$  error). Moreover there is a strong correlation between the retrieved and actual value of soil and vegetation moisture ( $R > 0.96$ ). Figure 7 shows the comparison between the retrieved and the actual soil moisture. A reference line is included for the ease of comparison between the retrieved and actual soil moisture.

Table 5. Retrieval results for soil and vegetation moisture.

Correlation Length	Noise Level	$m_v$		$v_{wc}$	
		RMSE	Corr (R)	RMSE	Corr (R)
Fixed (16 cm)	0 dB	0.024	0.980	0.001	0.990
Variable	0.5 dB	0.046	0.928	0.008	0.994

Table 6. Time taken for data cube generation and inversion algorithm.

Code	Number of points	Time taken (min.)
Data Cube Generation	1152	564
S-R Inversion	144	1.4

The simulations were run on an Intel Octa-Core i7 processor at 3.60 GHz with a RAM of 15.5 GB and the run time was noted as shown in the Table 6.

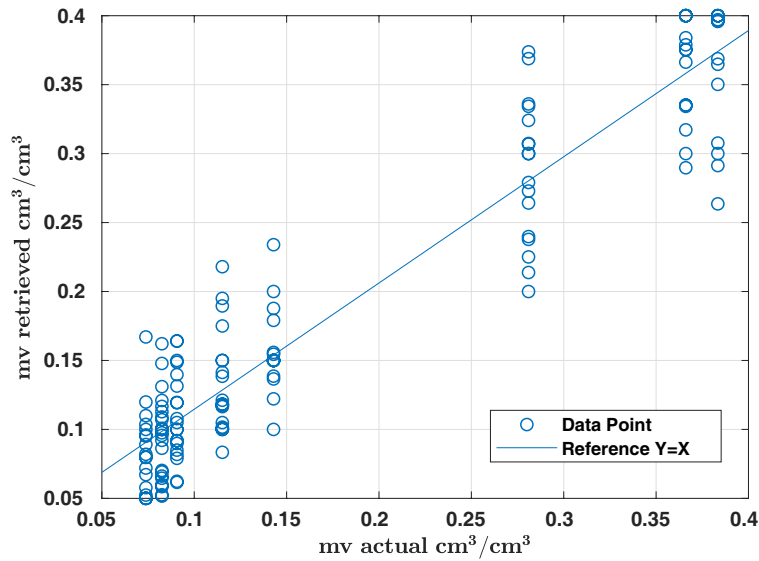


Figure 7. Comparison between retrieved and actual soil moisture.

## 5. CONCLUSION

In this paper, we presented an algorithm for retrieving soil moisture using a physics based forward model ( $I^2EM$ ) to generate backscatter. We extended the previous  $I^2EM$  model to incorporate depth dependency of moisture and included the effect of vegetation by modelling it as dielectric scatterers. The retrieval of soil and vegetation moisture was done using both single and dual bands; it was found that dual band retrievals yielded better results on expected lines. The results were found to be better than an existing inversion algorithm (SMART). The retrieval algorithm works with a good accuracy with RMSE being **0.046** for soil moisture and **0.008** for vegetation water content in case of vegetation. In future work, we will investigate the dependence of backscatter sensitivity to the soil and vegetation parameters and refine our retrieval algorithm accordingly methods to reduce the retrieval error further.

## ACKNOWLEDGMENT

The authors would acknowledge the Indian Space Research Organization — Space Applications Centre, for support via grant number ECO-13 titled “Soil Moisture Retrieval from Airborne Synthetic Aperture Radar” under the L&S band Airborne SAR RA. The authors also acknowledge helpful discussions on remote sensing with Prof. Harishankar Ramachandran.

## REFERENCES

- Entekhabi, D., E. G. Njoku, P. E. O’Neill, K. H. Kellogg, W. T. Crow, W. N. Edelstein, J. K. Entin, et al., “The soil moisture active passive (SMAP) mission,” *Proceedings of the IEEE*, Vol. 98, No. 5, 704–716, 2010.
- Kerr, Y. H., P. Waldteufel, J.-P. Wigneron, J. A. M. J. Martinuzzi, J. Font, and Michael Berger, “Soil moisture retrieval from space: The soil moisture and ocean salinity (SMOS) mission,” *IEEE Transactions on Geoscience and Remote Sensing*, Vol. 39, No. 8, 1729–1735, 2001.
- Petropoulos, G. P., G. Ireland, and B. Barrett, “Surface soil moisture retrievals from remote sensing: Current status, products & future trends,” *Physics and Chemistry of the Earth, Parts A/B/C*, Vol. 83, 36–56, 2015.
- Shi, J., J. Wang, A. Y. Hsu, P. E. O’Neill, and E. T. Engman, “Estimation of bare surface soil moisture and surface roughness parameter using L-band SAR image data,” *IEEE Transactions on Geoscience and Remote Sensing*, Vol. 35, No. 5, 1254–1266, 1997.
- Oh, Y., K. Sarabandi, and F. T. Ulaby, “An empirical model and an inversion technique for radar scattering from bare soil surfaces,” *IEEE transactions on Geoscience and Remote Sensing*, Vol. 30, No. 2, 370–381, 1992.
- Ulaby, F. T. and D. G. Long, *Microwave Radar and Radiometric Remote Sensing*, University of Michigan Press, 2014.

7. Fung, A. K., Z. Li, and K. S. Chen, “Backscattering from a randomly rough dielectric surface,” *IEEE Transactions on Geoscience and Remote Sensing*, Vol. 30, No. 2, 356–369, Mar 1992.
8. Dubois, P. C., J. Van Zyl, and T. Engman, “Measuring soil moisture with imaging radars,” *IEEE Transactions on Geoscience and Remote Sensing*, Vol. 33, No. 4, 915–926, 1995.
9. Hallikainen, M. T., F. T. Ulaby, M. C. Dobson, M. A. El-Rayes, and L.-K. Wu, “Microwave dielectric behavior of wet soil-part 1: Empirical models and experimental observations,” *IEEE Transactions on Geoscience and Remote Sensing*, Vol. 1, 25–34, 1985.
10. Fung, A. K., W. Y. Liu, K. S. Chen, and M. K. Tsay. “An improved IEM model for bistatic scattering from rough surfaces,” *Journal of Electromagnetic Waves and Applications*, Vol. 16, No. 5, 689–702, 2002.
11. Fung, A. K., et al., “A modified IEM model for: scattering from soil surfaces with application to soil moisture sensing,” *Geoscience and Remote Sensing Symposium, 1996. IGARSS’96. ‘Remote Sensing for a Sustainable Future’, International*, Vol. 2, 1297–1299, Lincoln, NE, 1996.
12. Van Zyl, J. J., *Synthetic Aperture Radar Polarimetry*, Vol. 2, John Wiley and Sons, 2011.
13. Ariei, M., “Retrieval of soil moisture under vegetation using polarimetric radar,” PhD Diss., California Institute of Technology, 2009.
14. Attema, E. P. W. and Fawwaz T. Ulaby, “Vegetation modeled as a water cloud,” *Radio Science*, Vol. 13, No. 2, 357–364, 1978.
15. Ulaby, F. T. and M. A. El-Rayes, “Microwave dielectric spectrum of vegetation-Part II: Dual-dispersion model,” *IEEE Transactions on Geoscience and Remote Sensing*, Vol. 5, 550–557, 1987.
16. Freeman, A. and S. L. Durden, “A three-component scattering model for polarimetric SAR data,” *IEEE Transactions on Geoscience and Remote Sensing*, Vol. 36, No. 3, 963–973, 1998.